Developmental Biology 366 (2012) 101–110

Contents lists available at SciVerse ScienceDirect

Developmental Biology

journal homepage: www.elsevier.com/locate/developmentalbiology

KLC3 is involved in sperm tail midpiece formation and sperm function

Ying Zhang [a], Young Ou [a], Min Cheng [a], Habib Shojaei Saadi [b], Jacob C. Thundathil [b], Frans A. van der Hoorn [a,*]

[a] Department of Biochemistry and Molecular Biology, Faculty of Medicine, University of Calgary, Calgary, Alberta, Canada T2N 4N1
[b] Department of Production Animal Health, Faculty of Veterinary Medicine, University of Calgary, Calgary, Alberta, Canada T2N 4N1

ARTICLE INFO

Article history:
Received 9 January 2012
Received in revised form
12 April 2012
Accepted 16 April 2012
Available online 27 April 2012

Keywords:
Spermatogenesis
Spermatid
Mitochondria
Kinesin
Transgenic mice

ABSTRACT

Kinesin light chain 3 (KLC3) is the only known kinesin light chain expressed in post-meiotic male germ cells. We have reported that in rat spermatids KLC3 associates with outer dense fibers and mitochondrial sheath. KLC3 is able to bind to mitochondria in vitro and in vivo employing the conserved tetratrico-peptide repeat kinesin light chain motif. The temporal expression and association of KLC3 with mitochondria coincides with the stage in spermatogenesis when mitochondria move from the spermatid cell periphery to the developing midpiece suggesting a role in midpiece formation. In fibroblasts, expression of KLC3 results in formation of large KLC3 aggregates close to the nucleus that contain mitochondria. However, the molecular basis of the aggregation of mitochondria by KLC3 and its role in sperm tail midpiece formation are not clear.

Here we show that KLC3 expression from an inducible system causes mitochondrial aggregation within 6 h in a microtubule dependent manner. We identified the mitochondrial outer membrane porin protein VDAC2 as a KLC3 binding partner. To analyze a role for KLC3 in spermatids we developed a transgenic mouse model in which a KLC3ΔHR mutant protein is specifically expressed in spermatids: this KLC3 mutant protein binds mitochondria and causes aggregate formation, but cannot bind outer dense fibers. Male transgenic mice display significantly reduced reproductive efficiency siring small sized litters. We observed defects in the mitochondrial sheath structure in a number of transgenic spermatids. Transgenic males have a significantly reduced sperm count and produce spermatozoa that exhibit abnormal motility parameters. Our results indicate that KLC3 plays a role during spermiogenesis in the development of the midpiece and in the normal function of spermatozoa.

Introduction

Spermatogenesis is characterized by continuous germ cell proliferation and differentiation and occurs in the seminiferous tubules of the testis. It can be divided into three stages. Spermiogenesis is the third and final stage during which the spermatid goes through an elaborate process of cyto-differentiation, producing the mature spermatozoon (Clermont et al., 1990). Among the major morphological changes that occur during spermiogenesis is the formation of the sperm tail (Oko and Clermont, 1990). The midpiece of the mammalian sperm tail is characterized by a mitochondrial helical sheath that surrounds the axonemal complex and the nine outer dense fibers (ODFs) (Fawcett, 1975).

Development of the mitochondrial sheath was studied since 1970, using different methods. It has been known that mitochondria of spermatogenic cells modify their morphological organization, number, and location and that the morphology of mitochondria changes from the original via a condensed form to the intermediate type (De et al., 1979; Meinhardt et al., 1999; Ho and Wey, 2007). The idea of mitochondria wrapping in a left-handed double helical structure was generally accepted. In recent years, several proteins that associate with spermatid mitochondria and ODFs have been identified, including sperm-associated antigens (Spags), Spetex-1, Tektins, et al. (Fitzgerald et al., 2006; Iida et al., 2006; Murayama et al., 2008). It is, however, still not fully understood how mitochondria in spermatids aggregate, and form the mitochondrial sheath around the ODF of the middle piece; there is little information on the function of molecules involved in this process.

Kinesins (KIF) are predominantly plus-end-directed microtubule (MT) motors. They are involved in the intracellular transport of organelles, protein complexes and mRNAs to specific destinations (Hirokawa et al., 2009). Specific kinesins can associate with and move mitochondria: purified KIF1B can transport mitochondria along microtubules in vitro (Nangaku et al., 1994); a KIF5B$^{-/-}$ knockout is embryonic-lethal in mice and causes perinuclear aggregation of mitochondria (Tanaka et al., 1998); selective inhibition of the interaction between RanBP2 and KIF5B/KIF5C in cell lines causes

* Correspondence to: Health Sciences Center, University of Calgary, 3330 Hospital Dr NW, Calgary, Alberta, Canada T2N 4N1. Fax: 403 210 8109.
E-mail address: fvdhoorn@ucalgary.ca (F.A. van der Hoorn).

0012-1606/$ - see front matter © 2012 Elsevier Inc. All rights reserved.
http://dx.doi.org/10.1016/j.ydbio.2012.04.026

perinuclear clustering of mitochondria (Cho et al., 2007). A specific isoform of rat kinesin light chain 1 (KLC1), called KLCb, binds mitochondria (Khodjakov et al., 1998); tumor necrosis factor causes hyperphosphorylation of KLC, impairs kinesin motor activity and results in perinuclear accumulation of mitochondria demonstrating that KLCs can be involved in mitochondrial transport (De Vos et al., 2000). Abnormal movement of mitochondria has been observed in human disorders such as Charcot-Marie-Tooth disease (CMT) 2A, Alzheimer's disease, Parkinson's disease, Huntington's disease, and Lou Gehrig's disease (Reynolds et al., 2004; Trimmer and Borland, 2005; Beal, 2007; Misko et al., 2010) could result from the dysfunction of kinesins.

KLCs are components of the kinesin I motor molecule that consists of two kinesin heavy chains (KHCs) associated with two KLCs. We reported the isolation of kinesin light chain 3 (KLC3) that is highly expressed in rat testis and accumulates in the sperm tail midpiece (Junco et al., 2001). KLC3 has domains characteristic of a typical KLC including the conserved heptad repeat (HR) that binds to KHC and five tetratricopeptide repeats (TPRs). We subsequently discovered that KLC3 can associate with ODFs via its HR domain (Bhullar et al., 2003) and with mitochondria via the TPR domain (Zhang et al., 2004). In rat testis, the association of KLC3 with mitochondria coincides with the stage in spermiogenesis when mitochondria move from the cell periphery to the developing midpiece. Expression of KLC3 in fibroblasts results in formation of large KLC3 clusters close to the nucleus, which also contain mitochondria. Our data suggested a role for KLC3 in spermatid midpiece formation. Here, we investigated the time course of aggregate formation as well as identify which mitochondrial protein may interact with KLC3. To analyze a role for KLC3 in spermatogenesis we used a transgenic mouse model to show that a KLC3 mutant protein incapable of binding ODF, but capable of binding mitochondria- adversely affects fertility and can cause midpiece abnormalities.

Materials & methods

Constructs used in this study:pGFP-KLC3 and pGFP-KLC3ΔHR mutant have been described before (Zhang et al., 2004). To generate RT7-KLC3ΔHR-GFP transgene plasmid, the pGFP-KLC3ΔHR vector was digested by SalI and cloned into RT7-GFP plasmid (van der Hoorn and Tarnasky, 1992). VDAC2 cDNA was made by RT-PCR using VDACf (5′ GGAATTCATGGCTGAATGTTGTGTACC 3′) and VDACr (5′ GCAGTCGACATTAAGGCCAAATCTTCTGAT 3′) primers. The PCR products were digested and cloned into a pci-HA vector. pTREGFP-KLC3 was made by digestion of pBS(ATG)KLC3 (Junco et al., 2001) with SalI and EcoRI restriction enzymes and cloning into the corresponding sites in the pTRE vector (Clontech) for Tet-On time course experiments.

Cell culture and transfection: NIH-3T3 cells were cultured in DMEM supplemented with 10% fetal bovine serum and 1% sodium pyruvate on 6-well plates containing glass coverslips. Cultures were transfected with the indicated GFP-KLC3 or HA-VDAC2 fusion constructs DNAs using Lipofectamine Plus reagent as recommended by the manufacturer. Cells were analyzed 48 h after transfection.

Preparation of germ cells and testis extracts: to investigate transgene expression in germ cells, freshly isolated transgenic testes were decapsulated to release seminiferous tubules. The seminiferous tubules were incubated in Krebs media (120 mM NaCl, 4.8 mM KCl, 25.2 mM $NaHCO_3$, 1.2 mM KH_2PO_4,1.2 mM $MgSO_4$, 1.3 mM $CaCl_2$, 0.25% BSA 1 mM Na Pyruvate, 6 mM Na Lactate) with 2 mg collagenase for 30 min at 32 °C followed by Krebs media with 0.125 mg/ml trypsin and DNAase I for 15 min. To the resulting single cell suspension we added 0.5 mg/ml trypsin inhibitor. Cells were stained with MitoTracker, fixed and analyzed by fluorescence confocal microscopy. Testis extracts from transgenic animals were prepared as described previously and analyzed by western blotting (Higgy et al., 1995).

Immunoprecipitations: pGFPKLC3 and pciHA-VDAC2 co-transfected NIH-3T3 cell extracts were prepared in lysis buffer (10 mM Tris pH 7.4, 150 mM NaCl, 10 mM KCl, 1 mM EDTA, 0.5% Deoxycholate, 0.5% Tween-20, 0.5% NP-40, 1 ug/ml aprotinin, 100 μg/ml PMSF). The protein extracts were pre-cleared by mixing with 20 μl protein G Sepharose beads and then incubated with 2 μl anti GFP antibodies (Sigma) and 50 μl 20% protein G beads for 4 h at 4 °C. Following incubation, beads were precipitated and washed three times with lysis buffer. SDS sample buffer was subsequently added to the beads to elute the protein sample which was used for gel electrophoresis followed by Western blotting.

Western blot analysis: Protein samples were boiled in sample buffer and resolved by SDS–PAGE followed by transfer onto nitrocellulose membrane (Amersham). The blots were blocked overnight in 1xTBS with 5% skim milk. Specific proteins on blots were analyzed by incubation with anti-HA (Sigma), anti-β-tubulin (Sigma) or anti KLC3 antibodies (Zhang et al., 2004), followed by horseradish peroxidase-coupled secondary antibodies (Sigma). Blots were developed using chemiluminescence (LumiGLO).

Immunofluorescence microscopy: Indirect immunofluorescence microscopy (IIF) was performed to localize proteins in transfected NIH-3T3 cells. Briefly, transfected or control NIH-3T3 cells grown on glass coverslips were fixed in 3.7% formaldehyde and permeabilized in 0.5% Triton X-100 (Sigma). Coverslips were incubated with primary antibodies (anti-HA) and then secondary antibodies (cy3 or cy5, Sigma) for 30 min at room temperature separately. Mitochondria were stained using MitoTracker red as described before (Zhang et al., 2004). Images were observed with a Zeiss confocal microscope.

KLC3 induction time course experiment: For the time course of GFP-KLC3 expression, NIH-3T3 cells were co-transfected with pTRE-GFP-KLC3 and the pTet-on vector using Lipofectamine Plus reagent (Invitrogen) as recommended by the manufacturer. After overnight incubation, doxycycline was added to the culture medium to a final concentration of 1 μM. GFP was observed by epifluorescence microscopy and images were taken at different time points, 1 h, 3 h, 6 h and 24 h. In indicated cases, nocodazole was added to the transfected cells to depolymerize MT. Nocodazole (Sigma) was dissolved in DMSO and added to the culture medium to a final concentration of 5.0 mM. Co-transfection and doxycycline treatments were done as described. Images of GFP were taken at 1 h, 3 h, 6 h and 3 days after doxycycline treatment.

Far western assay: Mitochondria were isolated as described before (Zhang et al., 2004). 5 μl isolated mitochondria were mixed with 2x SDS buffer and separated by denaturing SDS–PAGE. Separated proteins were transferred to nitrocellulose membranes. Blocking was performed with 2% skim milk in binding buffer (10% glycerol, 0.1 M NaCl, 0.02 M Tris pH 7.6, 1 mM EDTA, and 0.1% Tween-20) with 10 μM cold methionine overnight at 4 °C. Membranes were subsequently incubated with [^{35}S]-methionine labeled in vitro translated KLC3 or ODF1 (Zhang et al., 2004). The membrane was analyzed using autoradiography.

Generation of transgenic mice and breeding: the transgene RT7-KLC3ΔHR-GFP vector was digested with DraIII. The fragment, which has the KLC3ΔHR insert linked to a C-terminal GFP and the functional portion of the RT7 promoter, was cut out and the DNA was isolated using the Qiagen Gel Purification Kit (Qiagen). Purified DNA was used at the University of Calgary transgenic services for pronuclear injection to generate transgenic founders. Wild type CD1 mice were chosen for mating with founders. The litter size was counted.

Genomic PCR screening: 5 mm tail samples were collected from potential transgenic mice and incubated with 300 μl Direct PCR Lysis Reagent (Viagen Biotech) with 1.0 mg/ml Proteinase K overnight in a rotor at 55 °C. A 1 μl volume of supernatant was used as PCR template. Extended Long Template PCR (Roche) was performed using the Buffer 3 system. Forward primer transgene-F1 (5′ GTGGAAGTGAGAAGCTGGTCTC 3′) and reverse primer transgene-R3 (5′ ATGATCTTGTCGGTGAAGATCAC 3′) were used.

Analysis of transgenic testis: after genomic PCR screening and breeding, positive mice were sacrificed and testes were isolated. The whole testis and other organs were observed under the epifluorescence microscope for GFP signal. Testis protein extracts were prepared and western blotting was performed as described above using anti-KLC3 antibody. Testis from wild type CD1 mouse was used as a negative control. Isolated testes were cut into small piece and fixed in 4% PFA. The fixed tissues were rinsed in PBS 3 times and incubated in 10% sucrose for 6 h and subsequently in 25% sucrose overnight. Tissues were put into OCT compound in cryo-molds and placed at 4 °C for 1 h. Prepared molds were put in methanol cooled with dry ice until OCT froze completely. Tissue samples were sectioned using cryosectioning and put onto slides. GFP signal was visualized by confocal epifluorescence microscopy.

Transmission electron microscopy: testis samples were cut into approximately 1 mm cubes and fixed in 2.5% glutaraldehyde-PO_4 buffer for 1 h followed by 0.2 M osmium tetroxide for 30 min at room temperature. Fixed tissues were dehydrated in a graded ethanol series (25%, 35%, 50%, 75%, and 100%) for 10 min, respectively. The samples were then saturated with 1:3 (PolyBed 812 resin: 2-hydroxypropyl-methacrylate) for 30 min, 1:1 for 1 h, 3:1 for overnight and 100% resin for 3 h. Finally, the tissues were embedded in labeled capsules with fresh resin and polymerized at 60 °C for 48 h. The samples were sectioned and the ultra-thin sections were observed and photographed with a Hitachi-7650 microscope.

Computer Assisted Sperm Analysis (*CASA*): motion characteristics of the wild type sperm and sperm from KLC3ΔHR transgenic mice (age $\geq$10 weeks) were evaluated. In brief, the mice were euthanized by CD, cauda epididymides were carefully minced in 500 μl of pre-warmed (37 °C) TALPH buffer (NaCl 100 mM, KCl 3.1 mM, NaH_2PO_4, 0.3 mM, $MgCl_2$ 15 mM, Hepes 10 mM, Lactate 21.6 mM, EDTA 0.4 mM and 0.3% BSA, pH 7.4) and incubated for 10 min (37 °C). The sperm suspensions were collected and 4 μl of diluted sperm suspensions were loaded in 37 °C pre-warmed measuring slide (Leja, Nieuw-Vennep, The Netherlands) and seven fields per sample were analyzed based on recommendations by the manufacturer: 30 frames per objects; 60 Hz frame rate. Total motility, sperm concentration, straight line distance (DSL), average path velocity (VAP), straight line velocity (VSL), linearity (LIN), wobbelness (WOB) and straightness (STR), were recorded and the values were statistically compared between the groups using the *t*-test.

Results

Formation of large KLC3-mitochondrial clusters is rapid and microtubule dependent

We had previously shown that KLC3 expression in mouse fibroblasts causes mitochondrial clustering. This was based on observations of cells transfected for two or more days with GFP-KLC3 (Zhang et al., 2004). To follow cluster formation over time and to investigate the possible involvement of microtubules we designed a TET-inducible GFP-KLC3 NIH-3T3 cell expression system. The results of induction (Fig. 1) show that GFP-KLC3 initially shows a homogeneous cytoplasmic distribution (panel A), rapidly followed by formation of clusters (panel B) that become more intense within 6 h (panel C). Eventually clusters form very large aggregates (panel D). When the induction experiment was carried out in the presence of nocodazole, a microtubule destabilizing agent, small clusters formed that increased in intensity over time (panels E–G), but failed to form large aggregates even after several days (compare panels H and D). The effectiveness of the nocodazole treatment was verified by staining untreated and treated cells with anti-tubulin antibodies (Supplemental Fig. 1). We also observed that GFP-KLC3 localizes to the centrosome and primary cilium basal body when expressed at low levels (Supplemental Fig. 2). These experiments indicate that formation of large aggregates is rapid and requires microtubules.

VDAC2 is a candidate KLC3 binding partner

Our in vitro studies using radiolabeled KLC3 indicated that binding to mitochondria likely involves one or more mitochondrial or mitochondrion-associated proteins (Zhang et al., 2004). To identify possible mitochondrial binding partners of KLC3, we carried

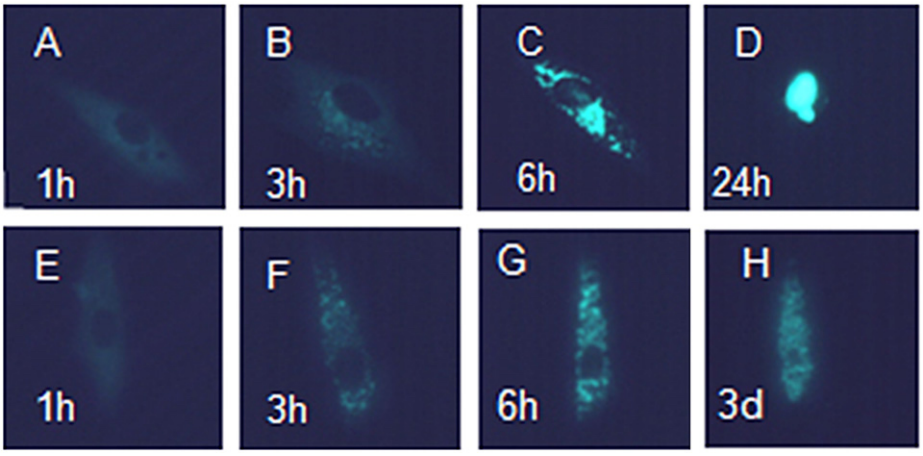

Fig. 1. KLC3-induced mitochondrial aggregate formation is microtubule-dependent. NIH-3T3 cells were co-transfected with pTREGFP-KLC3 and Tet-On vector. Twelve hours after transfection, doxycycline was added to cultures and cells were monitored by epifluorescence microscopy. Images were taken at various time points and examples are shown of the indicated time points after induction of GFP-KLC3. Panels A–D: GFP-KLC3 was induced and images taken at the indicated times of 1, 3, 6 and 24 h, respectively. Panels E–H: GFP-KLC3 was induced, and nocodazole was added to the cultures, and images taken at the indicated times of 1, 3, 6 and 72 h, respectively. Addition of nocodazole disrupted the ability of KLC3 to form aggregates.

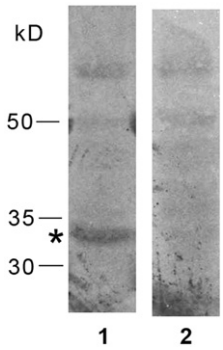

Fig. 2. Far western analysis. Mitochondrial lysates were separated by SDS–PAGE and transferred onto cellulose membranes. In vitro translated ^{35}S-radiolabeled KLC3 protein served as probe to analyze KLC3-binding proteins on the membrane. Lane 1: membrane incubated with radiolabeled KLC3. Lane 2: membrane incubated with radiolabeled ODF1 as negative control.

out far western assays of mitochondrial protein lysates separated by SDS–PAGE and transferred to nitrocellulose membranes. In vitro translated ^{35}S-labeled KLC3 protein served as a probe and was incubated with membranes. The results shown in Fig. 2 indicate that compared with the control (lane 2), a mitochondrial protein with an estimated molecular mass of 33 kDa binds to KLC3 (lane 1). Based on literature, this suggested the possibility that this protein may be (related to) voltage-dependent anion channel 2 (VDAC2) mitochondrial outer membrane porin.

To investigate this possibility, HA-tagged VDAC2 was co-transfected with GFP-KLC3 in NIH-3T3 cells. Cell lysates were analyzed by co-immunoprecipitation/western blotting assays. Immunoprecipitation was carried out using anti-GFP antibody and anti-HA antibody was used to detect HA-VDAC2 by western blotting in precipitates (Fig. 3A). The results show that HA-VDAC2 forms a complex with GFP-KLC3 (lanes 1 and 2; HA-VDAC2 indicated by the star). Lane 3 shows a control precipitation that lacked the GFP antibody demonstrating that the beads used in immunoprecipitation do not bind HA-VDAC2. Lane 4 shows a control experiment of cells transfected only with GFP-KLC3.

The expression and localization of VDAC2 protein was also investigated using immunofluorescence analysis of NIH-3T3 cells co-transfected with GFP-KLC3 and HA-VDAC2. The results (Fig. 3B) show that in cells expressing both GFP-KLC3 (green) and HA-VDAC2 (blue), these two proteins colocalize on aggregated mitochondria (red): the merged image shows white color where HA-VDAC2, GFP-KLC3 and mitochondria co-localize. Cells that only express HA-VDAC2 show HA-VDAC2 staining in the pattern of mitochondria (Fig. 3B, purple color in merged images). These results together identify VDAC2 as a mitochondrial protein that KLC3 binds to.

The KLC3ΔHR-GFP transgenic mouse model

The observations that KLC3 affects mitochondrial redistribution in somatic cells, binds the mitochondrial protein VDAC2 and is highly expressed during spermiogenesis at the time when mitochondria redistribute towards the midpiece in spermatids together support a model in which KLC3 plays a role in mitochondrial movement and sheath formation in the developing spermatid midpiece. Such a role cannot be investigated in isolated spermatids, which do not continue their developmental program in vitro. Therefore, we generated a transgenic mouse model that expresses a KLC3 deletion mutant under the control of the *Odf1* (formerly called RT7) promoter, which is a strong and spermatid-specific promoter that directs high levels of transgenic protein expression (Higgy et al., 1995). For this experiment we chose the KLC3ΔHR protein, which lacks the heptade repeat motif and does not bind ODF, but still associates with mitochondria and causes their clustering (Bhullar et al., 2003; Zhang et al., 2004). We linked KLC3ΔHR to GFP at its C-terminus. We hypothesized that if a sufficient level of expression of the KLC3ΔHR-GFP transgene can be obtained, KLC3ΔHR-GFP mutant protein will compete with wild type KLC3 for binding to mitochondria, but cannot bind ODF, possibly affecting midpiece morphogenesis and fertility. Several transgenic lines were obtained. Here we compare the results obtained from analysis of KLC3ΔHR-GFP transgenic lines 16 and 18, which differ significantly in the level of KLC3ΔHR-GFP mutant protein expression, with wild type mice.

KLC3ΔHR-GFP expression in the testis of transgenic mice

To confirm KLC3ΔHR-GFP expression and compare protein levels in lines 16 and 18, testes from transgenic mice were first analyzed for GFP expression by epifluorescence microscopy. KLC3ΔHR-GFP fluorescence was detected in testes of transgenic mouse lines 16 (Fig. 4). Line 16 male mice and their offspring showed high levels of transgene expression in the seminiferous tubules of the testis (panels A and D). Transgene expression is restricted to spermatids. As a result of the cycle of the seminiferous epithelium different parts of the seminiferous tubules contain cells at different stages of spermatogenesis and consequently are expected to show different numbers of spermatids and consequently levels of GFP: variation in GFP intensity along tubules was indeed observed (Fig. 4). In contrast to line 16, a much lower level of KLC3ΔHR-GFP fluorescence was detected in seminiferous tubules in the testes of line 18 males and their offspring (panels B and E). Fluorescence could not be detected above background in any transgenic female mice (not shown), or in other tissues of male mice of lines 16 and 18 including heart, brain and kidney and liver (panel C). No significant differences were found in the size or weight of testes from lines 16 and 18 compared to wild type mice. To confirm the fluorescence KLC3ΔHR-GFP expression results, testis protein extracts from wild type mice and from lines 16 and 18 and their offspring were analyzed by western blotting using anti-GFP antibody. All transgenic mice showed detectable levels of KLC3ΔHR-GFP protein (Fig. 4, panel F, lanes 2–5), which protein was absent from control mice as expected (lane 1). The expression levels in testes from line 16 and offspring (lanes 2 and 4, respectively) appear significantly higher than in testes from line 18 and offspring (lanes 3 and 5, respectively), in agreement with the GFP epifluorescence observations (compare panels A and B). Anti-β-tubulin antibody was used as control for protein amount and quality (panel F). Together these data indicate that the KLC3ΔHR-GFP transgene was successfully expressed in transgenic male mice in adult testis.

To confirm that GFP expression within seminiferous tubules is restricted to spermatids, testis sections from transgenic lines 16 were analyzed for GFP. Testis from wild type CD1 was used as negative control. GFP signal was visualized by confocal fluorescence microscopy (Fig. 5). The Odf1 promoter drives KLC3ΔHR-GFP transgene expression in postmeiotic male germ cells (panels A and B), as expected (Higgy et al., 1995). The GFP signal in transgenic adult testis was abundant in the cytoplasm of spermatids (panels D and E show image overlays with differential interference contrast (DIC) images of the same sections). No GFP signal was observed in seminiferous tubules of wild type mice (panels C and F). Panels A and B also show that the tails of elongating spermatids contain small amounts of KLC3ΔHR-GFP protein. To further analyze protein expression in transgenic spermatids we used immunofluorescence analysis of total male germ cell preparations of line 16 testes and found that KLC3ΔHR-GFP in

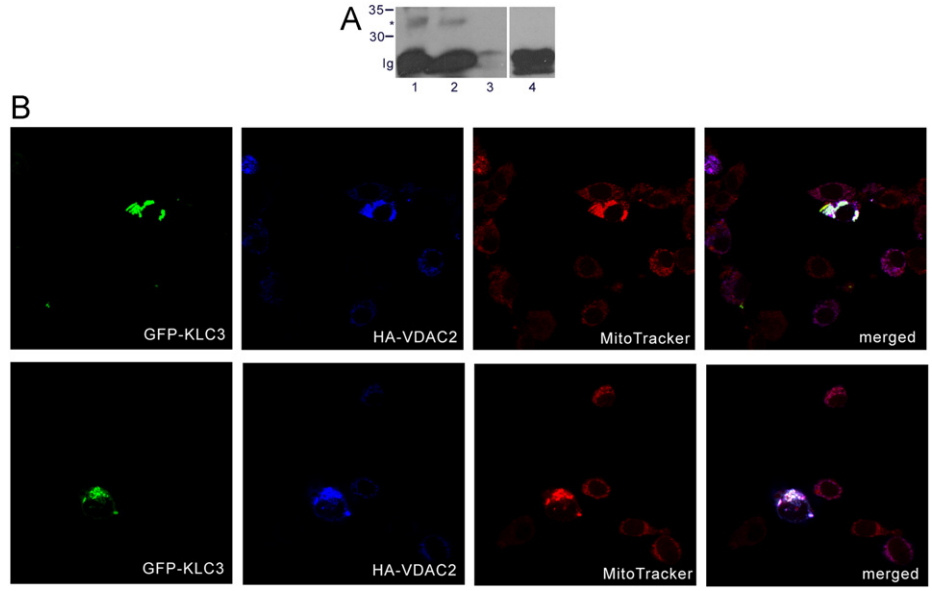

Fig. 3. KLC3 binds mitochondrial VDAC2 protein. Panel A: NIH-3T3 cells were co-transfected with pHA-VDAC2 and GFP-KLC3 (lanes 1 – 3) or with GFP-KLC3 only (lane 4). Cell lysates were collected and immunoprecipitation was carried out using anti-GFP antibody (lanes 1, 2 and 4). Lysate in lane 3 received only beads used for the immunoprecipitation as negative control. Anti-HA antibody was used in western blotting of complexes to detect HA-VDAC2 in precipitates. Panel B: the expression and localization of HA-VDAC2 protein were investigated using immunofluorescence analysis of NIH-3T3 cells co-transfected with HA-VDAC2 and GFP-KLC3. Transfected cells were also stained with MitoTracker (red). GFP signal (green) was observed by fluorescence microscopy. HA-VDAC2 signal (blue) was visualized using anti-HA antibodies in indirect immunofluorescence microscopy. Merged images show colocalization of all three signals in aggregated mitochondria, as white color.

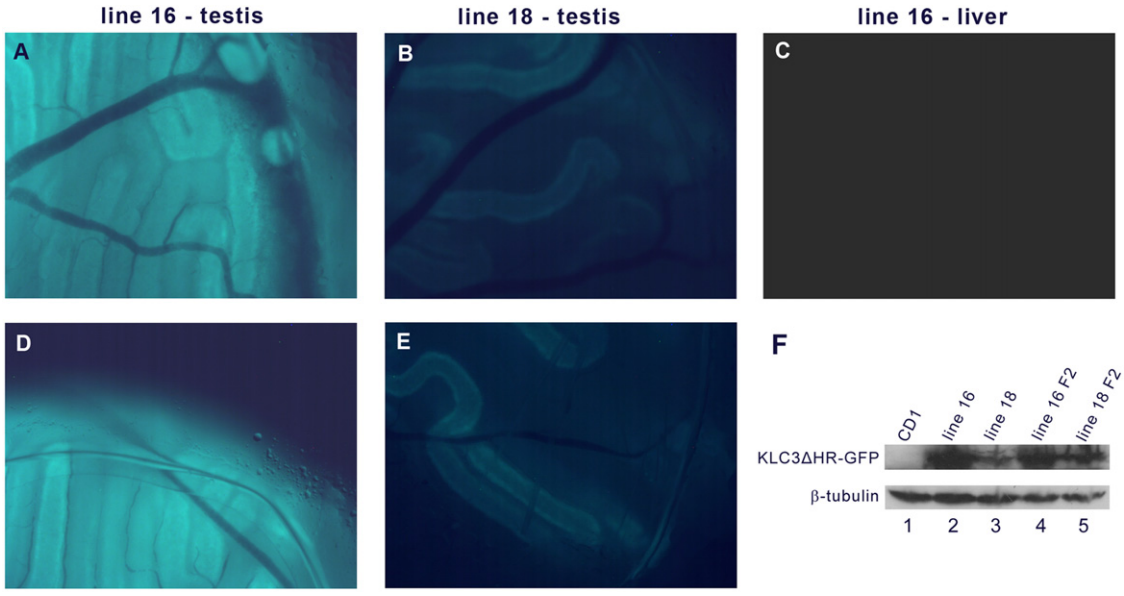

Fig. 4. KLC3ΔHR-GFP expression in testes of transgenic lines 16 and 18. Testes from transgenic mouse lines 16 and 18 carrying the KLC3ΔHR-GFP transgene were analyzed for GFP expression by epifluorescence microscopy at 2–3 months of age. Line 16 males (panel A) and F2 offspring (panel D) showed high levels of transgene expression in seminiferous tubules. Line 18 males (panel B) and F2 offspring (panel E) showed low level expression of the transgene in seminiferous tubules. Fluorescence was not detected above background levels in other tissues of male line 16 mice (panel C, liver). F: Testis protein extracts from line 16 (lanes 2 and 4), line 18 (lanes 3 and 5) and wild type CD1 males (lane 1) mice were analyzed for expression of the 81 kD KLC3ΔHR-GFP protein by western blotting using GFP antibodies. Anti-β-tubulin antibodies were used as control.

transgenic spermatids appeared to co-localize with some, but not all, mitochondria (Fig. 6: yellow color in merged images).

KLC3ΔHR-GFP transgenic mice are subfertile

We next analyzed the fertility of the transgenic lines, by mating wild type female CD1 mice to transgenic males of lines 16 and 18 (founders and several generations of offspring). Litter size was determined and tail biopsies were collected after weaning to determine transgene status. Table 1 summarizes the breeding results. Transgenic mice of line 16 display a significantly reduced fertility, consistently producing only small litters (average 3–4 pups) in over 20 matings using different generations of line 16 male mice. Transgenic mice of line 18 produced litter sizes similar to those of wild type mice (average 12–13 pups). This indicated that males of line 16, but not of line 18, are subfertile.

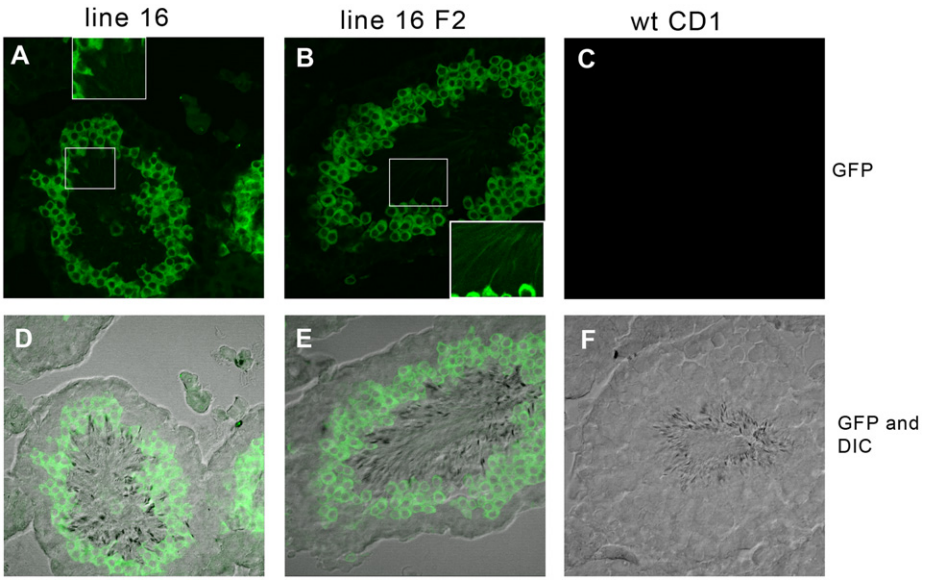

Fig. 5. KLC3ΔHR-GFP expression in testis sections. Testis sections from KLC3ΔHR-GFP transgenic line 16 F1 (A, D) and line 16 F2 (B, E) were analyzed for GFP signal. Testes from wild type CD1 male were used as control (C, F). GFP signal was visualized by confocal epifluorescence microscopy and DIC images were taken subsequently. Panel D, E and F show merged images for GFP signal and DIC. Transgene expression is restricted to postmeiotic male germ cells. The insets show enlarged regions as indicated visualizing the very low level expression of the transgene in sperm tails.

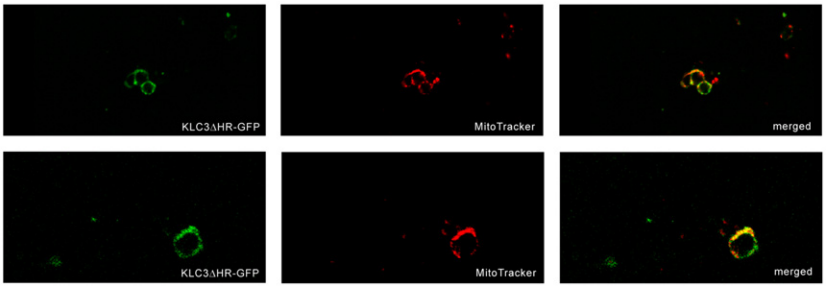

Fig. 6. KLC3ΔHR-GFP colocalizes with mitochondria in transgenic spermatids. Total seminiferous tubule cell preparations from line 16 transgenic males were analyzed for KLC3ΔHR-GFP protein expression by fluorescence microscopy (green). Mitochondria in the cells were labeled with MitoTracker (red). Merged images show that KLC3ΔHR-GFP signal overlaps with some, but not all, mitochondria.

Table 1
Litter size from KLC3ΔHR-GFP transgenic males mated to wild type CD1 females.

Transgenic line	Line 16	Line 18
Founder male	$5.3 \pm 1.5^{a,b}$	$12.5 \pm 0.5^{a,b}$
F1 males	$4.0 \pm 0.5^{a,c}$	$13.0 \pm 0.5^{a,c}$
F2 males	2.8 ± 0.8^{a}	ND

[a] Average number of pups per litter.
[b] Difference in average litter size is statistically significant (pValue < 0.05).
[c] Difference in average litter size is statistically significant (pValue < 0.05).

Elongating spermatids of KLC3ΔHR-GFP transgenic mice can exhibit midpiece abnormalities

To investigate the possibility that KLC3ΔHR-GFP mutant protein expression caused morphological defects in developing spermatids, we analyzed midpieces of line 16 spermatids and wild type spermatids by electron microscopy (Fig. 7). In wild type mice, the single mitochondrial layer of the developing midpiece was distributed evenly around ODF to form the mitochondrial sheath (Fig. 7, panel A). In line 16 spermatids, we observed a majority of spermatids that appeared to have a normal midpiece as well as cases of spermatids exhibiting several types of midpiece abnormalities: multiple layers of mitochondria (panel B); mitochondria unevenly distributed around ODF (panel C) and single malformed mitochondria (panel D, arrow; a normal midpiece is present at the top right corner of this panel). Based on all EM observations we estimate that 5–10% of transgenic spermatids have an abnormality in the forming midpiece region. Epididymal sperm of line 16 males lacked these abnormalities (not shown).

KLC3ΔHR-GFP transgenic spermatozoa: reduced sperm count and abnormal motility parameters

Midpiece abnormalities and the presence—albeit at a low level—of the KLC3ΔHR-GFP mutant protein in sperm tails, may affect the number and functionality of spermatozoa. We measured sperm count and sperm motility characteristics for line 16 males in comparison to wild type CD1 mice. Spermatozoa were collected from cauda epididymides and analyzed using Computer Assisted Sperm Analysis. Total sperm count was reduced in line 16 males to 72% of the sperm count of wild type males (Table 2). In addition, several motility parameters showed significant differences between spermatozoa of wild type and line 16 mice (Table 2). The average value of straight line velocity (VSL) in line 16 was 44.05, which was significantly below that of wild type spermatozoa (65.9, $P < 0.05$). Values for DSL (straight line distance), VAP (average path velocity), WOB (wobble), LIN

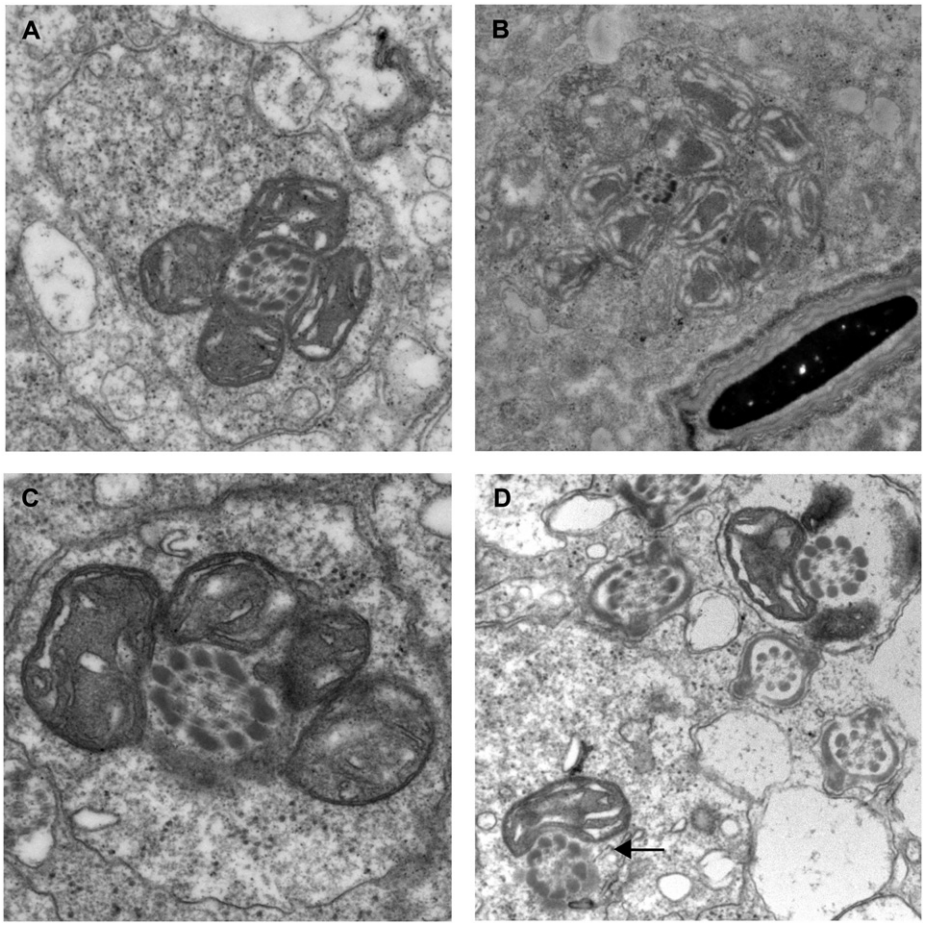

Fig. 7. Mitochondrial sheath defects in elongating KLC3ΔHR-GFP transgenic spermatids. Testis from adult transgene line 16 males (panels B–D) and wild type CD1 males (panel A) were fixed in glutaraldehyde and post-fixed in osmium tetroxide. Tissues were dehydrated, embedded in Epon resin and sectioned. Ultra-thin sections were observed and photographed with a Hitachi-7650 microscope. In wild type CD1 mice a single mitochondrial layer is evenly distributed around outer dense fibers forming the mitochondria sheath (panel A). In transgenic line 16 mice we observed in addition to a majority of normal looking midpieces (panel D, top right corner) several examples of abnormally forming mitochondrial sheath structures during midpiece formation, including multi-layered mitochondrial sheaths (panel B), unevenly distributed mitochondrial arrangements around the outer dense fibers (panel C) and midpieces containing a single mitochondrion (panel D, arrow). Forming heads (panel B) and principal pieces (panel D) appeared normal.

Table 2
CASA analysis of sperm motility parameters.

Parameter	Wild type	Line 16	*p* Value
Motility (%)	50.9 ± 2.4	49.12 ± 1.9	> 0.05
Sperm count (million)	3.6 ± 0.2	2.6 ± 0.12	< 0.05
VAP (microns/second)	85.5 ± 4.0	68.65 ± 3.6	< 0.05
WOB	0.53 ± 0.02	0.48 ± 0.03	< 0.05
VSL (microns/second)	65.9 ± 4.2	44.05 ± 3.5	< 0.05
DSL (microns)	29.3 ± 1.4	19.95 ± 1.5	< 0.05
LIN	0.41 ± 0.03	0.30 ± 0.02	< 0.05
STR	0.76 ± 0.04	0.63 ± 0.03	< 0.05

(linearity) and STR (straightness) were also significantly lower in line 16 mice compared to wild type ($P < 0.05$). Sperm with STR values over 75% and LIN values over 35% are considered progressively motile (Defoin et al., 2008; Jimenez et al., 2011). The STR and LIN values for line 16 males (0.63 and 0.30, respectively; Table 2) suggest that progressive motility of line 16 sperm is adversely affected. We did not observe significant differences in the motility characteristics DCL (distance of curve line), DAP (distance of average path), BCF (beat cross frequency), ALH (amplitude of lateral head displacement) and VCL (velocity of curve line). These data suggest that a reduced sperm count and/or changes in motility characteristics of spermatozoa in KLC3ΔHR-GFP transgenic mice may have contributed to the observed reduced fertility.

Discussion

KLC3 is the only known kinesin light chain expressed in post-meiotic male germ cells which suggested a unique role for KLC3 during spermiogenesis. In this study, we observed that KLC3 can cause clustering of mitochondria in a microtubule-dependent fashion causing aggregate formation and binds the mitochondrial protein VDAC2. Transgenic mice expressing high levels of the KLC3ΔHR mutant protein display reduced fertility siring small sized litters. Transgenic mice expressing high levels of KLC3ΔHR had a significantly reduced sperm count; some spermatids show abnormal midpiece development and spermatozoa displayed abnormal motility parameters compared to wild type mice. Our results suggest that KLC3 plays a role during the formation of sperm tail midpiece and in sperm function.

Mitochondrial outer membrane porin protein VDAC2 binds KLC3

Kinesins typically use scaffold proteins and adapter proteins to bind to cargo. However, some kinesins can also directly bind to membrane proteins of cargo. The adapter proteins syntabulin

(Cai et al., 2005), Ran-binding protein 2 (RanBP2) (Cho et al., 2007) and the Milton-Miro complex (Rice and Gelfand, 2006) were independently identified as mediators of mitochondrial binding to KIF5 motors. However, the relationship between many kinesins and adapters that regulate mitochondrial distribution is poorly understood. In addition to adapter proteins, lipids also contribute to the specificity of cargo binding. KIF1A and KIF16B employ the PH domains in their tail regions to specifically bind to phosphatidylinositides such as PIP_2 and PIP_3, respectively (Klopfenstein et al., 2002; Hoepfner et al., 2005). KIF13B binds indirectly to PIP_3 via the PH domain of β-centaurin (Venkateswarlu et al., 2005). We investigated the possible binding between KLC3 and lipids. However, our results did not provide any indication that KLC3 can bind a lipid (data not shown).

Our results demonstrated that VDAC2 present on mitochondria binds to KLC3. VDAC2 is one of three VDAC proteins in mammals. In testis, it is mainly present in late spermatocytes and spermatids, and is abundant in ODFs of bovine spermatozoa (Triphan et al., 2008; Liu et al., 2009; Menzel et al., 2009). Our co-immunoprecipitation and immunofluorescence results showed that VDAC2-KLC3 complexes exist in co-transfected cells. However, we do not know if the interaction is direct or mediated by another protein. Although our far western result indicate that binding can be direct, it was recently shown that caytaxin binds to the TPR domain of kinesin light chain proteins, including KLC3, and can function as an adapter that mediates intracellular transport of specific cargos, one of which is the mitochondrion (Aoyama et al., 2009). It is therefore possible that caytaxin binds to mitochondria via mitochondrial membrane proteins (such as VDAC2) and tethers them to KLC3 or other kinesins for transport. Preliminary results from co-transfection experiments (Supplemental Fig. 3) suggest that KLC3 can compete with the mitochondrial associated kinesin KIF1B for binding to mitochondria: in transfected cells KIF1B associates with mitochondria (panel 1–3). KLC3 co-expression dislodges KIF1B from mitochondria and is now found at the cell periphery (panels 4–7). It is not yet known if KIF1B binds VDAC2, but a recent observation suggests that kinesin can indeed associate with the mitochondrial VDAC proteins (Yang et al., 2011).

KLC3ΔHR transgenic mice display reduced fertility

In view of the fact that KLC3 is predominantly expressed in elongating spermatids and becomes associated with mitochondria at the time when mitochondria move from the cell periphery to the developing midpiece below the condensing nucleus, and our observation that it induces mitochondrial aggregation in cultured cells (Zhang et al., 2004), we proposed that KLC3 may be involved in spermiogenesis by assisting the formation of the mitochondrial sheath in the midpiece of spermatozoa. Precisely regulated mitochondrial sheath formation is critical for sperm motility and fertility (Ramalho-Santos et al., 2009). Although a recent paper suggested that sperm mitochondrial integrity is not required for hyperactivated motility in the rhesus macaque (Hung et al., 2008), several knockout mouse models that have specific anomalies of the sperm mitochondrial sheath result in sperm motility disorders (Escalier, 2006a; Escalier, 2006b). Male knockout mice such as Gopc$^{-/-}$ and Nectin-2$^{-/-}$ are infertile partly due to defects in mitochondrial sheath development during spermiogenesis (Bouchard et al., 2000; Suzuki-Toyota et al., 2004).

To investigate a role for KLC3 in spermiogenesis, we generated transgenic mouse lines that express *Klc3Δhr* linked to GFP under the control of the *Odf1* promoter (formerly called RT7). The *Odf1* promoter is strong and testis-specific (Higgy et al., 1995). The KLC3ΔHR protein was chosen because it does not bind ODF but still associates with mitochondria and causes their aggregation (Zhang et al., 2004). We hypothesized that KLC3ΔHR expression in transgenic round spermatids may compete with wild type KLC3 and interfere with the normal association of mitochondria with ODF affecting normal midpiece and mitochondrial sheath development that occurs from step 14 onwards. We obtained mouse lines with low and with high levels of transgenic protein expression in testis, specifically in postmeiotic male germ cells, and compared their fertility, spermatid development and sperm motility characteristics with wild type male mice. Males of transgenic lines expressing high levels of KLC3ΔHR display reduced fertility: when mated to wild type females, few offspring (small litters) were produced. We observed defects in the mitochondrial sheath structure in some transgenic spermatids, which included multiple layers of mitochondria; single mitochondrion and unevenly distributed mitochondria around ODF. Similar phenotypes had been observed by Wilton: mitochondria in spermatozoa from two infertile patients were disorganized and many are clustered in the proximal region of the midpiece (Wilton et al., 1992). Of course, it remains to be shown if KLC3 was involved in those phenotypes. High expressing KLC3ΔHR transgenic mice produced caudal spermatozoa with an apparently normal phenotype. However, sperm count was significantly reduced, which may result from the inability of spermatids with a malformed midpiece to mature into spermatozoa or from other effects including increased apoptosis. Preliminary results using the TUNEL assay to detect apoptotic cells suggest an increased level of apoptosis in testes of line 16 mice compared to wild type mice (Supplemental Fig. 4, panels C and A, respectively), but we do not know if this contributes significantly to the observed decrease in sperm count, which requires further investigation.

Caudal spermatozoa from mice expressing high levels of the KLC3ΔHR transgene display abnormalities in motility parameters, indicative of reduced progressive motility. A significant decline in straight linear velocity, average path velocity, straightness, and linearity indicated that KLC3ΔHR severely affected not only the ability of spermatozoa to move in a forward direction but also affected their vigor. We did not observe a significant change in ALH, suggesting that once attached to an egg transgenic sperm should be able to penetrate the zona pellucida. We observed that tails of transgenic spermatozoa contain small amounts of KLC3ΔHR mutant protein, which may affect mitochondrial function. The possible effect of the transgenic protein on sperm motility parameters remains to be determined.

Model for KLC3's role in spermatids

Fig. 8 presents schematically a model for KLC3 action in elongating spermatids that incorporates our current knowledge about KLC3 as well as results from other groups on VDAC2 and kinesins that bind mitochondria. After meiosis, mitochondria are located near the cell periphery of early spermatids. It is possible that they are held in that position by kinesin. At later stages in spermiogenesis KLC3 protein expression significantly increases (elongating spermatids). Our preliminary data suggest that KLC3 causes KIF1B kinesin to dislodge from mitochondria. Mitochondria that are released from kinesin may move toward the center of the cell possibly in association with dynein. The possible involvement of dynein in the transport and localization of mitochondria is lend support by observations in Drosophila where the absence of the cytoplasmic dynein heavy chain cDhc leads to abnormal clustering and jamming of mitochondria with evidence of interdependency of dynein and kinesin in fast axonal transport (Martin et al., 1999). Axonemal microtubules are surrounded by ODF and not accessible to KLC3-coated mitochondria at that stage. Once KLC3-coated mitochondria have moved from the periphery to the developing midpiece, KLC3 is proposed to act as an anchor protein bringing mitochondria and ODF together: the HR region of KLC3 interacts with the leucine zipper

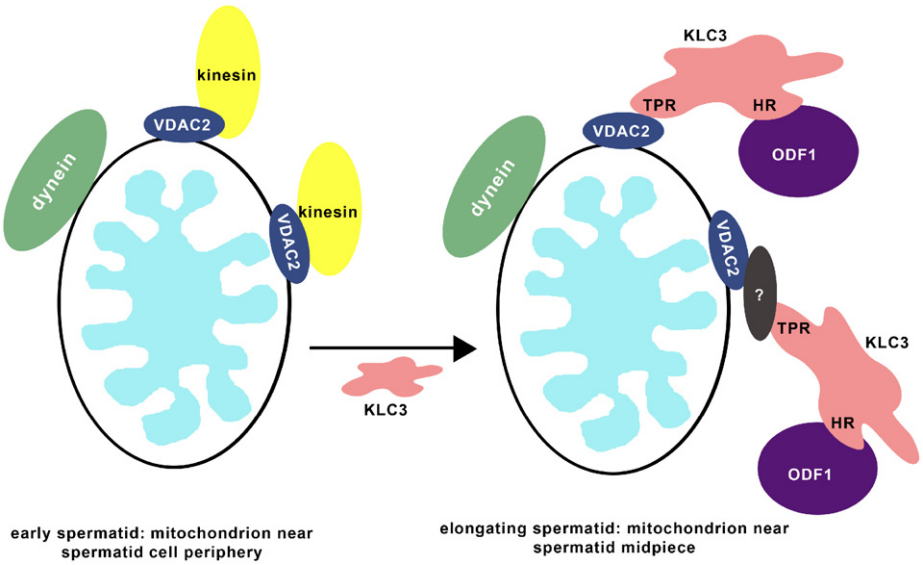

Fig. 8. A model for KLC3 function in spermatids. Our model proposes that in early spermatids mitochondria are located close to the cell periphery in association with dynein and kinesin. Kinesin binds to VDAC2. During later stages of spermiogenesis KLC3 becomes abundantly expressed. KLC3 is proposed to disengage kinesin from the mitochondria resulting in their dynein-mediated movement towards the ODF in the developing midpiece. The KLC3 TPR region can be associated directly with mitochondria (VDAC2) or through an adapter (e.g. caytaxin). In elongating spermatids KLC3 could act as bridging molecule between mitochondria and ODF: the KLC3 HR region is known to interact with the ODF protein ODF1 and KLC3 has been observed by immuno-EM between mitochondria and ODF.

domain of ODF protein ODF1. The TPR region can associate with mitochondrial outer membrane protein VDAC2 directly or through an adapter (possibly caytaxin). In the case of high level expression of the KLC3ΔHR mutant protein, which cannot bind to the kinesin heavy chain (Junco et al., 2001), aggregation will occur but not in a timely fashion coordinated with assembly on the ODF of the forming midpiece. Although we do not yet know if one KLC3 molecule can simultaneously engage with both a mitochondrion and an ODF, in support of this possibility we have observed KLC3 protein localized between ODFs and mitochondria (Zhang et al., 2004).

Acknowledgments

YZ was the recipient of a Canadian Institutes of Health Research (CIHR) doctoral studentship. The authors gratefully acknowledge the technical assistance of H. Tarnasky with transgenic experiments. This work was supported by grants from CIHR to FAvdH, and from the Natural Sciences and Engineering Research Council of Canada to JT.

Appendix A. Supporting information

Supplementary data associated with this article can be found in the online version at http://dx.doi.org/10.1016/j.ydbio.2012.04.026.

References

Aoyama, T., Hata, S., Nakao, T., Tanigawa, Y., Oka, C., Kawaichi, M., 2009. Cayman ataxia protein caytaxin is transported by kinesin along neurites through binding to kinesin light chains. J. Cell Sci. 122, 4177–4185.

Beal, M.F., 2007. Mitochondria and neurodegeneration. Novartis. Found. Symp. 287, 183–192.

Bhullar, B., Zhang, Y., Junco, A., Oko, R., van der Hoorn, F.A., 2003. Association of Kinesin light chain with outer dense fibers in a microtubule-independent fashion. J. Biol. Chem. 278, 16159–16168.

Bouchard, M.J., Dong, Y., McDermott Jr., B.M., Lam, D.H., Brown, K.R., Shelanski, M., Bellve, A.R., Racaniello, V.R., 2000. Defects in nuclear and cytoskeletal morphology and mitochondrial localization in spermatozoa of mice lacking nectin-2, a component of cell–cell adherens junctions. Mol. Cell Biol. 20, 2865–2873.

Cai, Q., Gerwin, C., Sheng, Z.H., 2005. Syntabulin-mediated anterograde transport of mitochondria along neuronal processes. J. Cell Biol. 170, 959–969.

Cho, K.I., Cai, Y., Yi, H., Yeh, A., Aslanukov, A., Ferreira, P.A., 2007. Association of the kinesin-binding domain of RanBP2 to KIF5B and KIF5C determines mitochondria localization and function. Traffic 8, 1722–1735.

Clermont, Y., Oko, R., Hermo, L., 1990. Immunocytochemical localization of proteins utilized in the formation of outer dense fibers and fibrous sheath in rat spermatids: an electron microscope study. Anat. Rec. 227, 447–457.

De Vos, K., Severin, F., Van Herreweghe, F., Vancompernolle, K., Goossens, V., Hyman, A., Grooten, J., 2000. Tumor necrosis factor induces hyperphosphorylation of kinesin light chain and inhibits kinesin-mediated transport of mitochondria [In Process Citation]. J. Cell Biol. 149, 1207–1214.

De, M.C., Floridi, A., Marcante, M.L., Malorni, W., Scorza, B.P., Bellocci, M., Silvestrini, B., 1979. Morphological, histochemical and biochemical studies on germ cell mitochondria of normal rats. Cell Tissue Res. 196, 1–22.

Defoin, L., Granados, A., Donnay, I., 2008. Analysing motility parameters on fresh bull semen could help to predict resistance to freezing: a preliminary study. Reprod. Domest. Anim. 43, 606–611.

Escalier, D., 2006a. Knockout mouse models of sperm flagellum anomalies. Hum. Reprod. Update 12, 449–461.

Escalier, D., 2006b. [Animal models: Candidate genes for human male infertility]. Gynecol. Obstet. Fertil. 34, 827–830.

Fawcett, D.W., 1975. The mammalian spermatozoon. Dev. Biol. O 44, 394–436.

Fitzgerald, C.J., Oko, R.J., van der Hoorn, F.A., 2006. Rat Spag5 associates in somatic cells with endoplasmic reticulum and microtubules but in spermatozoa with outer dense fibers. Mol. Reprod. Dev. 73, 92–100.

Higgy, N.A., Zackson, S.L., van der Hoorn, F.A., 1995. Cell interactions in testis development: overexpression of c-mos in spermatocytes leads to increased germ cell proliferation. Dev. Genet. 16, 190–200.

Hirokawa, N., Nitta, R., Okada, Y., 2009. The mechanisms of kinesin motor motility: lessons from the monomeric motor KIF1A. Nat. Rev. Mol. Cell Biol. 10, 877–884.

Ho, H.C., Wey, S., 2007. Three dimensional rendering of the mitochondrial sheath morphogenesis during mouse spermiogenesis. Microsc. Res. Technol. 70, 719–723.

Hoepfner, S., Severin, F., Cabezas, A., Habermann, B., Runge, A., Gillooly, D., Stenmark, H., Zerial, M., 2005. Modulation of receptor recycling and degradation by the endosomal kinesin KIF16B. Cell 121, 437–450.

Hung, P.H., Miller, M.G., Meyers, S.A., VandeVoort, C.A., 2008. Sperm mitochondrial integrity is not required for hyperactivated motility, zona binding, or acrosome reaction in the rhesus macaque. Biol. Reprod. 79, 367–375.

Iida, H., Honda, Y., Matsuyama, T., Shibata, Y., Inai, T., 2006. Spetex-1: a new component in the middle piece of flagellum in rodent spermatozoa. Mol. Reprod. Dev. 73, 342–349.

Jimenez, T., Sanchez, G., McDermott, J.P., Nguyen, A.N., Kumar, T.R., Blanco, G., 2011. Increased expression of the Na,K-ATPase alpha4 isoform enhances sperm motility in transgenic mice. Biol. Reprod. 84, 153–161.

Junco, A., Bhullar, B., Tarnasky, H.A., van der Hoorn, F.A., 2001. Kinesin light-chain KLC3 expression in testis is restricted to spermatids. Biol. Reprod. 64, 1320–1330.

Khodjakov, A., Lizunova, E.M., Minin, A.A., Koonce, M.P., Gyoeva, F.K., 1998. A specific light chain of kinesin associates with mitochondria in cultured cells. Mol. Biol. Cell 9, 333–343.
Klopfenstein, D.R., Tomishige, M., Stuurman, N., Vale, R.D., 2002. Role of phosphatidylinositol(4,5)bisphosphate organization in membrane transport by the Unc104 kinesin motor. Cell 109, 347–358.
Liu, B., Wang, Z., Zhang, W., Wang, X., 2009. Expression and localization of voltage-dependent anion channels (VDAC) in human spermatozoa. Biochem. Biophys. Res. Commun. 378, 366–370.
Martin, M., Iyadurai, S.J., Gassman, A., Gindhart Jr., J.G., Hays, T.S., Saxton, W.M., 1999. Cytoplasmic dynein, the dynactin complex, and kinesin are interdependent and essential for fast axonal transport. Mol. Biol. Cell. 10, 3717–3728.
Meinhardt, A., Wilhelm, B., Seitz, J., 1999. Expression of mitochondrial marker proteins during spermatogenesis. Hum. Reprod. Update 5, 108–119.
Menzel, V.A., Cassara, M.C., Benz, R., de, P., Messina, V, Cunsolo, A., Saletti, V., Hinsch, R., Hinsch, E., K.D., 2009. Molecular and functional characterization of VDAC2 purified from mammal spermatozoa. Biosci. Rep. 29, 351–362.
Misko, A., Jiang, S., Wegorzewska, I., Milbrandt, J., Baloh, R.H., 2010. Mitofusin 2 is necessary for transport of axonal mitochondria and interacts with the Miro/Milton complex. J. Neurosci. 30, 4232–4240.
Murayama, E., Yamamoto, E., Kaneko, T., Shibata, Y., Inai, T., Iida, H., 2008. Tektin5, a new Tektin family member, is a component of the middle piece of flagella in rat spermatozoa. Mol. Reprod. Dev. 75, 650–658.
Nangaku, M., Sato-Yoshitake, R., Okada, Y., Noda, Y., Takemura, R., Yamazaki, H., Hirokawa, N., 1994. KIF1B, a novel microtubule plus end-directed monomeric motor protein for transport of mitochondria. Cell 79, 1209–1220.
Oko, R., Clermont, Y., 1990. Mammalian spermatozoa: structure and assembly of the tail. In: Gagnon, C. (Ed.), Controls of Sperm Motilty: Biological and Clinical Aspects. CRC Press Inc., Boca Raton, FL, pp. 3–27.
Ramalho-Santos, J., Varum, S., Amaral, S., Mota, P.C., Sousa, A.P., Amaral, A., 2009. Mitochondrial functionality in reproduction: from gonads and gametes to embryos and embryonic stem cells. Hum. Reprod. Update 15, 553–572.
Reynolds, I.J., Malaiyandi, L.M., Coash, M., Rintoul, G.L., 2004. Mitochondrial trafficking in neurons: a key variable in neurodegeneration? J. Bioenerg. Biomembr. 36, 283–286.
Rice, S.E., Gelfand, V.I., 2006. Paradigm lost: milton connects kinesin heavy chain to miro on mitochondria. J. Cell Biol. 173, 459–461.
Suzuki-Toyota, F., Ito, C., Toyama, Y., Maekawa, M., Yao, R., Noda, T., Toshimori, K., 2004. The coiled tail of the round-headed spermatozoa appears during epididymal passage in GOPC-deficient mice. Arch. Histol. Cytol. 67, 361–371.
Tanaka, Y., Kanai, Y., Okada, Y., Nonaka, S., Takeda, S., Harada, A., Hirokawa, N., 1998. Targeted disruption of mouse conventional kinesin heavy chain, kif5B, results in abnormal perinuclear clustering of mitochondria. Cell 93, 1147–1158.
Trimmer, P.A., Borland, M.K., 2005. Differentiated Alzheimer's disease transmitochondrial cybrid cell lines exhibit reduced organelle movement. Antioxid. Redox. Signal. 7, 1101–1109.
Triphan, X., Menzel, V.A., Petrunkina, A.M., Cassara, M.C., Wemheuer, W., Hinsch, K.D., Hinsch, E., 2008. Localisation and function of voltage-dependent anion channels (VDAC) in bovine spermatozoa. Pflugers Arch. 455, 677–686.
van der Hoorn, F.A., Tarnasky, H.A., 1992. Factors involved in regulation of the RT7 promoter in a male germ cell derived in vitro transcription system. Proc. Natl. Acad. Sci. USA 89, 703–707.
Venkateswarlu, K., Hanada, T., Chishti, A.H., 2005. Centaurin-alpha1 interacts directly with kinesin motor protein KIF13B. J. Cell Sci. 118, 2471–2484.
Wilton, L.J., Temple-Smith, P.D., de Kretser, D.M., 1992. Quantitative ultrastructural analysis of sperm tails reveals flagellar defects associated with persistent asthenozoospermia. Hum. Reprod. 7, 510–516.
Yang, X.Y., Chen, Z.W., Xu, T., Qu, Z., Pan, X.D., Qin, X.H., Ren, D.T., Liu, G.Q., 2011. Arabidopsis kinesin KP1 specifically interacts with VDAC3, a mitochondrial protein, and regulates respiration during seed germination at low temperature. Plant Cell. 23, 1093–1106.
Zhang, Y., Oko, R., van der Hoorn, F.A., 2004. Rat kinesin light chain 3 associates with spermatid mitochondria. Dev. Biol. 275, 23–33.